Supporting Information

Neonectrolide A, a New Oxaphenalenone Spiroketal from the Fungus *Neonectria* sp.

Jinwei Ren,[†,Δ] Fan Zhang,[†,Δ] Xiangyu Liu,[‡] Li Li,[§] Gang Liu,*[,†] Xingzhong Liu,[†] and Yongsheng Che*[,⊥]

State Key Laboratory of Mycology, Institute of Microbiology, Chinese Academy of Sciences, Beijing 100190, People's Republic of China, College of Resources & Environment, Huazhong Agricultural University, Wuhan 430070, People's Republic of China, Institute of Materia Medica, Chinese Academy of Medical Sciences & Peking Union Medical College, Beijing 100050, People's Republic of China, and Beijing Institute of Pharmacology & Toxicology, Beijing 100850, People's Republic of China

Contents **Page**

---

* To whom correspondence should be addressed. Tel/Fax: +86 10 66932679. E-mail: (Y.C.) cheys@im.ac.cn; (G.L.) liug@im.ac.cn.

† Institute of Microbiology.

‡ Huazhong Agricultural University.

§ Institute of Materia Medica.

⊥ Beijing Institute of Pharmacology & Toxicology.

Δ Contributed equally to this work.

Experimental Section

General Experimental Procedures. Optical rotations were measured on a Rodolph Research Analytical Automatic Polarimeter, and UV data were obtained on a Unico UV-2802H spectrophotometer. CD spectra were recorded on a JASCO J-815 spectropolarimeter. IR data were recorded using a Nicolet Magna-IR 750 spectrophotometer. ^{1}H and ^{13}C NMR data were acquired with Bruker Avance-500 and Varian INOVA-500 NMR spectrometers using solvent signals ($CDCl_3$: δ_H 7.28/δ_C 77.0; acetone-d_6: δ_H 2.05/δ_C 29.8, 206.1) as references. The HMQC and HMBC experiments were optimized for 145.0 and 8.0 Hz, respectively. ESIMS and HRESIMS data were obtained using an Agilent Accurate-Mass-Q-TOF LC/MS 6520 instrument equipped with an electrospray ionization (ESI) source. The fragmentor and capillary voltages were kept at 125 and 3500 V, respectively. Nitrogen was supplied as the nebulizing and drying gas. The temperature of the drying gas was set at 300 °C. The flow rate of the drying gas and the pressure of the nebulizer were 10 L/min and 10 psi, respectively. All MS experiments were performed in positive ion mode. Full-scan spectra were acquired over a scan range of *m/z* 100–1000 at 1.03 spectra/s. HPLC separations were performed on an Agilent 1200 instrument (Agilent, USA) equipped with a variable wavelength UV detector.

Fungal Material. The culture of *Neonectria* sp. (Nectriaceae) was isolated from a soil sample collected from Qinghai-Tibetan plateau (N: 28°27′, E: 97°02′), Chayu, Tibet, People's Republic of China, in May, 2004. The isolate was identified by Ms. Manman Wang based on morphology and sequence (Genbank Accession No. JX566703) analysis of the ITS region of the rDNA, and assigned the accession number XZ010 in X.L.'s culture

collection at the Institute of Microbiology, Chinese Academy of Sciences, Beijing. The fungal strain was cultured on slants of potato dextrose agar (PDA) at 15 °C for 10 days. Agar plugs were cut into small pieces (about 0.5 × 0.5 × 0.5 cm^3) under aseptic conditions and 15 of these pieces were used to inoculate in three Erlenmeyer flasks (250 mL), each containing 50 mL of media (0.4% glucose, 1% malt extract, and 0.4% yeast extract; the final pH of the media was adjusted to 6.5 and sterilized by autoclave). Three flasks of the inoculated media were incubated at 15 °C on a rotary shaker at 170 rpm for five days to prepare the seed culture. Fermentation was carried out in 12 Fernbach flasks (500 mL) each containing 80 g of rice. Distilled H_2O (120 mL) was added to each flask, and the contents were soaked overnight before autoclaving at 15 psi for 30 min. After cooling to room temperature, each flask was inoculated with 5.0 mL of the spore inoculum and incubated at 15 °C for 40 days.

Extraction and Isolation. The fermented material was extracted repeatedly with EtOAc (4 × 2.4 L), and the organic solvent was evaporated to dryness under vacuum to afford the crude extract (12.4 g), which was fractionated by silica gel Vacuum Liquid Chromatography (VLC) using PE–EtOAc–MeOH gradient elution. The fraction (363 mg) eluted with 100:55 PE–EtOAc was separated by Sephadex LH-20 column chromatography (CC) eluting with 1:1 CH_2Cl_2–MeOH, and the resulting subfractions were further purified by semipreparative RP HPLC (Agilent Zorbax SB-C_{18} column; 5 μm; 9.4 × 250 mm; 80% MeOH in H_2O for 2 min, followed by 80–85% MeOH over 35 min; 2 mL/min) to afford **1** (1.7 mg, t_R 25.31 min). The fraction (374 mg) eluted with 100:80 PE–EtOAc was separated by Sephadex LH-20 CC eluting with MeOH, and the resulting subfractions were

purified by RP HPLC (75% MeOH in H_2O for 2 min, followed by 75–90% MeOH over 40 min; 2 mL/min) to afford **2** (2.5 mg, t_R 43.28 min). The fraction (370 mg) eluted with 40:100 PE–EtOAc was purified by RP HPLC (10% CH_3CN in H_2O for 2 min, followed by 10–35% CH_3CN over 40 min; 2 mL/min) to afford **3** (34 mg, t_R 24.15 min).

Neonectrolide A (1): pale yellow powder; $[\alpha]^{16.7}_D$ –4.6 (*c* 0.13, MeOH); UV (MeOH) λ_{max} (log ε) 220 (1.20), 229 (1.21), 265 (0.67), 273 (0.93), 339 (0.26) nm; CD (*c* 4.40 × 10^{-4} M, MeOH) λ_{max} ($\Delta\varepsilon$) 225 (+0.58), 248 (+7.98), 276 (–4.45), 338 (–3.00) nm; IR (neat) ν_{max} 3735, 2969, 2934, 1738, 1664, 1616, 1455, 1366, 1297, 1242, 1204, 1179, 1119, 1062 cm^{-1}; ^1H, ^{13}C NMR, and HMBC data see Table 1; NOESY correlations ($CDCl_3$, 500 MHz) H-3 ↔ H-4′; H_2-7′ ↔ H-3′, H-4′; H-9′ ↔ H-5′; H-6 ↔ H_3-13; H_3-12 ↔ H-9, H_3-13; HRESIMS *m/z* 477.1525 (calcd. for $C_{25}H_{26}O_8Na$, 477.1520).

Corymbiferan lactone E (2): yellow powder; UV (MeOH) λ_{max} (log ε) 219 (4.06), 232 (4.12), 267 (4.1037), 344 (3.57), 360 (3.53) nm; IR (neat) ν_{max} 3423, 2934, 1627, 1458, 1410, 1376, 1304, 1212, 1172, 1130 cm^{-1}; ^1H NMR (acetone-d_6, 500 MHz) δ 11.99 (1H, s, OH-10), 10.12 (1H, s, OH-5), 6.76 (1H, s, H-9), 6.60 (1H, s, H-6), 5.62 (2H, s, H_2-3), 3.91 (3H, s, H_3-13), 2.77 (3H, s, H_3-12); ^{13}C NMR (acetone-d_6, 125 MHz) δ 170.3 (qC, C-1), 162.8 (qC, C-10), 159.0 (qC, C-7), 153.1 (qC, C-5), 147.0 (qC, C-8,), 132.9 (qC, C-11a), 116.8 (CH, C-9), 112.3 (qC, C-7a), 99.2 (qC, C-4), 96.9 (qC, C-11), 96.3 (CH, C-6), 66.7 (CH_2, C-3), 55.0 (CH_3,C-13), 24.8 (qC, C-12); HMBC data (acetone-d_6, 500 MHz) H_2-3 → C-1, 4, 5, 11a; H-6 → 4, 5, 7, 7a; H-9 → 7a, 10, 11, 12; H_3-12 → 7a, 8, 9; OH-10→9, 10, 11; HRESIMS *m/z* 261.0755 (calcd. for $C_{14}H_{13}O_5$, 261.0763).

3-Dehydroxy-4-*O*-acetylcephalosporolide C (3): colorless oil; $[\alpha]^{16.7}_D$ +44.0 (*c* 0.2,

MeOH); UV (MeOH) λ_{max} (log ε) 209 (2.45), 273 (1.58); IR (neat) ν_{max} 3435, 2975, 2954, 2934, 1729, 1438, 1377, 1361, 1300, 1247, 1214, 1130, 1061 cm^{-1}; ^1H NMR ($CDCl_3$, 500 MHz) δ 5.45 (1H, m, H-4), 5.08 (1H, m, H-9), 2.71 (1H, d, J = 4.5 Hz, H-5a), 2.69 (1H, br s, H-5b), 2.53 (1H, m, H-2a), 2.41 (1H, m, H-2b), 2.37 (1H, m, H-7a), 2.30 (1H, m, H-7b), 2.27 (1H, m, H-3a) 2.12 (1H, m, H-8a), 2.02 (3H, s, H_3-12), 2.00 (1H, m, H-8b), 1.81 (1H, m, H-3b), 1.23 (3H, d, J = 6.5 Hz, H_3-10); ^{13}C NMR ($CDCl_3$, 125 MHz) δ 208.4 (qC, C-6), 172.1 (qC, C-1), 170.0 (qC, C-11), 72.0 (CH, C-9), 69.0 (CH, C-4), 44.7 (CH_2, C-5), 39.8 (CH_2, C-7), 34.2 (CH_2, C-8), 28.2 (CH_2, C-2), 24.4 (CH_2, C-3), 21.2 (CH_3, C-12), 19.52 (CH_3, C-10); HMBC data ($CDCl_3$, 500 MHz) H-2 → C-1, 3, 4; H-5 → C-3, 4, 6, 7; H-9 → C-1, 7, 8; H-10 → C-8, 9; NOED data ($CDCl_3$, 500 MHz) H-9 ↔ H-7a, H_2-8, H_3-10; H-4 ↔ H_2-3, H_2-5,H-7b; HRESIMS *m/z* 265.1056 (calcd. for $C_{12}H_{18}O_5Na$, 265.1052).

Deacetylation of 3-Dehydroxy-4-*O*-acetylcephalosporolide C (3). A solution of **3** (5 mg) in 1 mL NaOH–MeOH (pH = 11) was stirred at 60 °C for 1 h, diluted with aqueous formic acid, and then extracted with $CHCl_3$. The $CHCl_3$ solution was concentrated and the residue purified by preparative TLC using 1:1 PE–EtOAc to afford the deacetylation product **5** (3.2 mg; *m/z* 201.1121 $[M + H]^+$).

Preparation of (*R*)- (5a) and (*S*)-MTPA (5b) Esters. A sample of **5** (1.6 mg, 0.008 mmol), (*S*)-MPTA Cl (5.0 μL, 0.026 mmol), and pyridine-d_5 (0.5 mL) were allowed to react in an NMR tube at ambient temperature for 12 h. The mixture was purified by RP HPLC (Agilent Zorbax SB-C_{18} column; 5 μm; 9.4 × 250 mm; 55% MeOH in H_2O for 2 min, followed by 55–100% MeOH over 33 min) to afford **5a** (1.8 mg, t_R 30.74 min); ^1H NMR ($CDCl_3$, 500 MHz) δ 5.15 (1H, m, H-9), 4.89 (1H, m, H-4), 2.92 (1H, ddd, J = 17.5, 6.0, 1.5

Hz, H-5a), 2.65 (1H, m, H-5b), 2.56 (2H, m, H_2-2), 2.49 (2H, m, H_2-7), 2.47 (1H, m, H-3a), 1.98 (1H, m, H-8a), 1.88 (1H, m, H-8b), 1.88 (1H, m, H-3b), 1.30 (3H, d, J = 6.5 Hz, H_3-10).

Similarly, a sample of **5** (1.6 mg, 0.008 mmol), (*R*)-MPTA Cl (5.0 μL, 0.026 mmol), and pyridine-d_5 (0.5 mL) were allowed to react in an NMR tube at ambient temperature for 12 h, and the reaction mixture was processed as described above for **5a** to afford **5b** (2.7 mg); ^{1}H NMR ($CDCl_3$, 500 MHz) δ 5.16 (1H, m, H-9), 4.87 (1H, m, H-4), 2.85 (1H, dd, J = 17.0, 6.5 Hz, H-5a), 2.57 (1H, m, H-5b), 2.58 (2H, m, H_2-2), 2.48 (1H, m, H-3a), 2.35 (2H, m, H_2-7), 1.95 (1H, m, H-8a), 1.88 (1H, m, H-3b), 1.84 (1H, m, H-8b), 1.40 (3H, d, J = 6.0 Hz, H_3-10).

Computational Details. Systematic conformational analyses for **4** were performed via the Molecular Operating Environment (MOE) ver. 2009.10. (Chemical Computing Group, Canada) software package using the MMFF94 molecular mechanics force field calculation. The MMFF94 conformational analyses were further optimized using TDDFT at B3LYP/6-31G(d) basis set level. The stationary points have been checked as the true minima of the potential energy surface by verifying they do not exhibit vibrational imaginary frequencies. The 40 lowest electronic transitions were calculated and the rotational strengths of each electronic excitation were given using both dipole length and dipole velocity representations. ECD spectra were stimulated using a Gaussian function with a half-bandwidth of 0.3 eV. Equilibrium populations of conformers at 298.15 K were calculated from their relative free energies (ΔG) using Boltzmann statistics. The overall ECD spectra were then generated according to Boltzmann weighting of each conformer. The systematic errors in the prediction of the wavelength and excited-state energies are

compensated for by employing UV correlation. All quantum computations were performed using Gaussian03 package,[1] on an IBM cluster machine located at the High Performance Computing Center of Peking Union Medical College.

MTS Assay.[2] The assay was run in triplicate. In a 96-well plate, each well was plated with (2–5) × 10^3 cells (depending on the cell multiplication rate). After cell attachment overnight, the medium was removed, and each well was treated with 100 μL medium containing 0.1% DMSO, or appropriate concentrations of the test compounds and the positive control cisplatin (100 mM as stock solution of a compound in DMSO and serial dilutions; the test compounds showed good solubility in DMSO and did not precipitate when added to the cells). The plate was incubated for 48 h at 37 °C in a humidified, 5% CO_2 atmosphere. Proliferation was assessed by adding 20 μL of MTS (Promega) to each well in the dark, followed by a 90 min incubation at 37 °C. The assay plate was read at 490 nm using a microplate reader. The inhibition was calculated and plotted versus test concentrations to afford the IC_{50}.

References:

1. Frisch, M. J.; Trucks, G. W.; Schlegel, H. B.; Scuseria, G. E.; Robb, M. A.; Cheeseman, J. R.; Montgomery, Jr., J. A.; Vreven, T.; Kudin, K. N.; Burant, J. C.; Millam, J. M.; Iyengar, S. S.; Tomasi, J.; Barone, V.; Mennucci, B.; Cossi, M.; Scalmani, G.; Rega, N.; Petersson, G. A.; Nakatsuji, H.; Hada, M.; Ehara, M.; Toyota, K.; Fukuda, R.; Hasegawa, J.; Ishida, M.; Nakajima, T.; Honda, Y.; Kitao, O.; Nakai, H.; Klene, M.; Li, X.; Knox, J. E.; Hratchian, H. P.; Cross, J. B.; Bakken, V.; Adamo, C.; Jaramillo, J.; Gomperts, R.;

Stratmann, R. E.; Yazyev, O.; Austin, A. J.; Cammi, R.; Pomelli, C.; Ochterski, J. W.; Ayala, P. Y.; Morokuma, K.; Voth, G. A.; Salvador, P.; Dannenberg, J. J.; Zakrzewski, V. G.; Dapprich, S.; Daniels, A. D.; Strain, M. C.; Farkas, O.; Malick, D. K.; Rabuck, A. D.; Raghavachari, K.; Foresman, J. B.; Ortiz, J. V.; Cui, Q.; Baboul, A. G.; Clifford, S.; Cioslowski, J.; Stefanov, B. B.; Liu, G.; Liashenko, A.; Piskorz, P.; Komaromi, I.; Martin, R. L.; Fox, D. J.; Keith, T.; Al-Laham, M. A.; Peng, C. Y.; Nanayakkara, A.; Challacombe, M.; Gill, P. M. W.; Johnson, B.; Chen, W.; Wong, M. W.; Gonzalez, C.; and Pople, J. A. *Gaussian 03, Revision E. 01*; Gaussian, Inc., Wallingford CT, 2004.

2. Zhang, N.; Chen, Y.; Jiang, R.; Li, E.; Chen, X.; Xi, Z.; Guo, Y.; Liu, X.; Zhou, Y.; Che, Y.; Jiang, X. *Autophagy* **2011**, *7*, 598–612.

Figure S1. ^{1}H NMR Spectrum of Neonectrolide A (**1**; 500 MHz, $CDCl_3$)

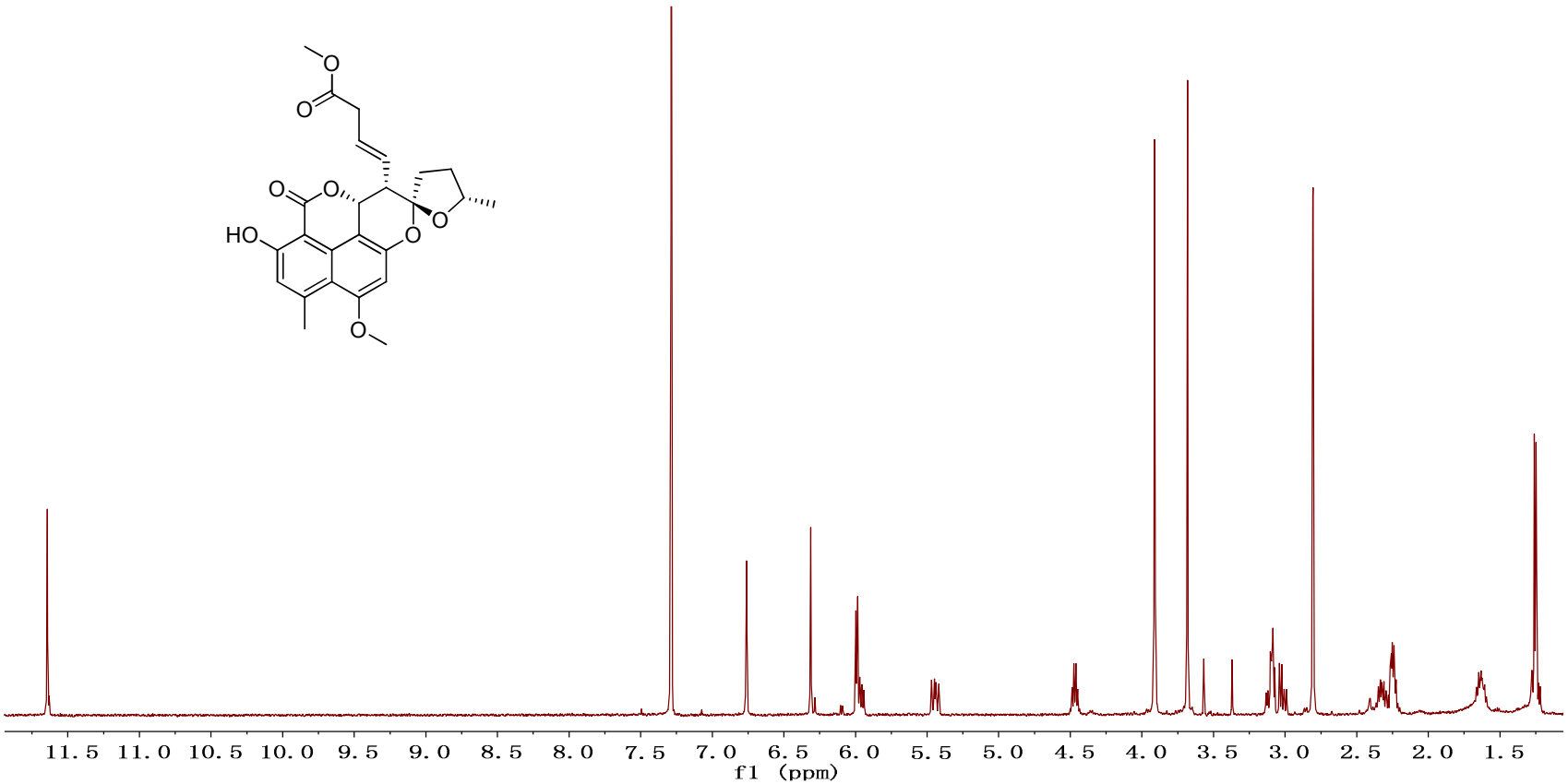

Figure S2. ^{13}C APT NMR Spectrum of Neonectrolide A (**1**; 125 MHz, $CDCl_3$)

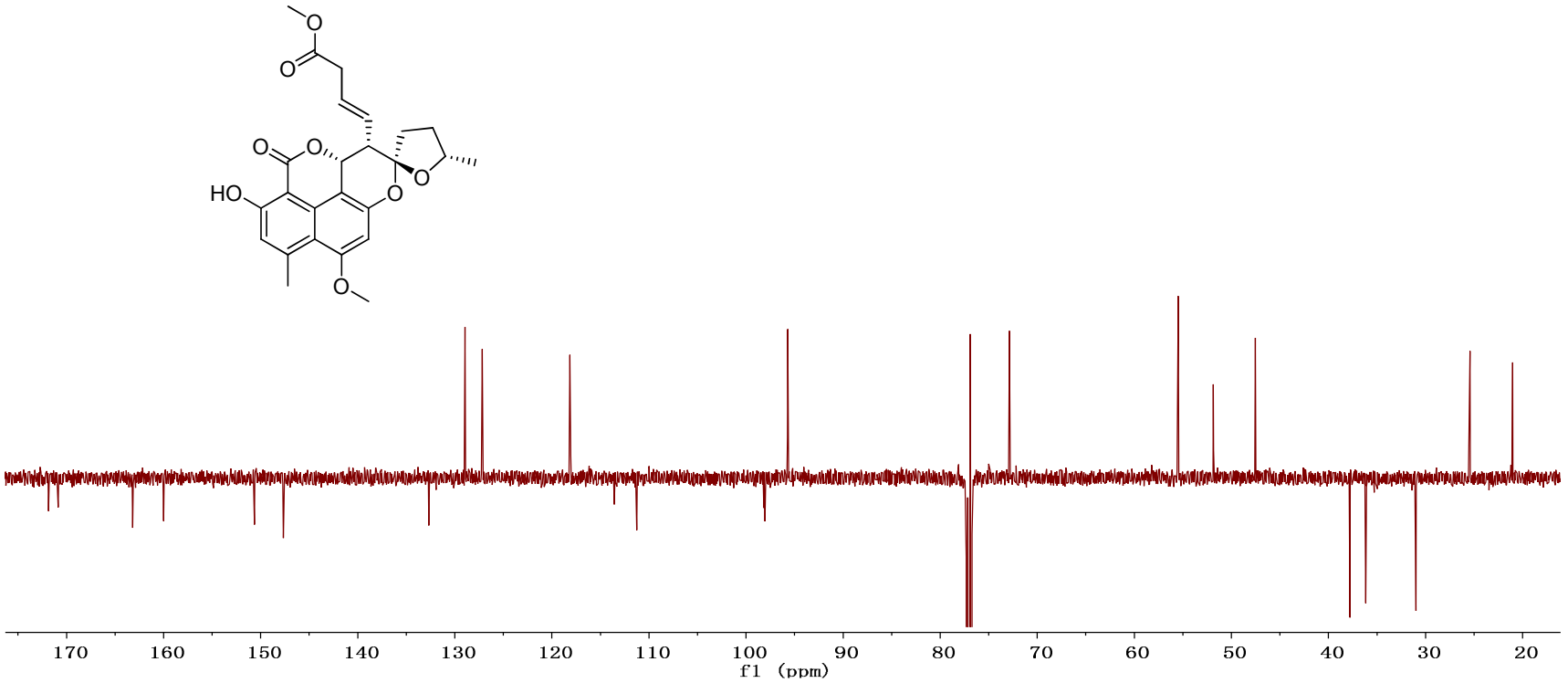

Figure S3. $^{1}H–^{1}H$ COSY Spectrum of Neonectrolide A (**1**; 500 MHz, $CDCl_3$)

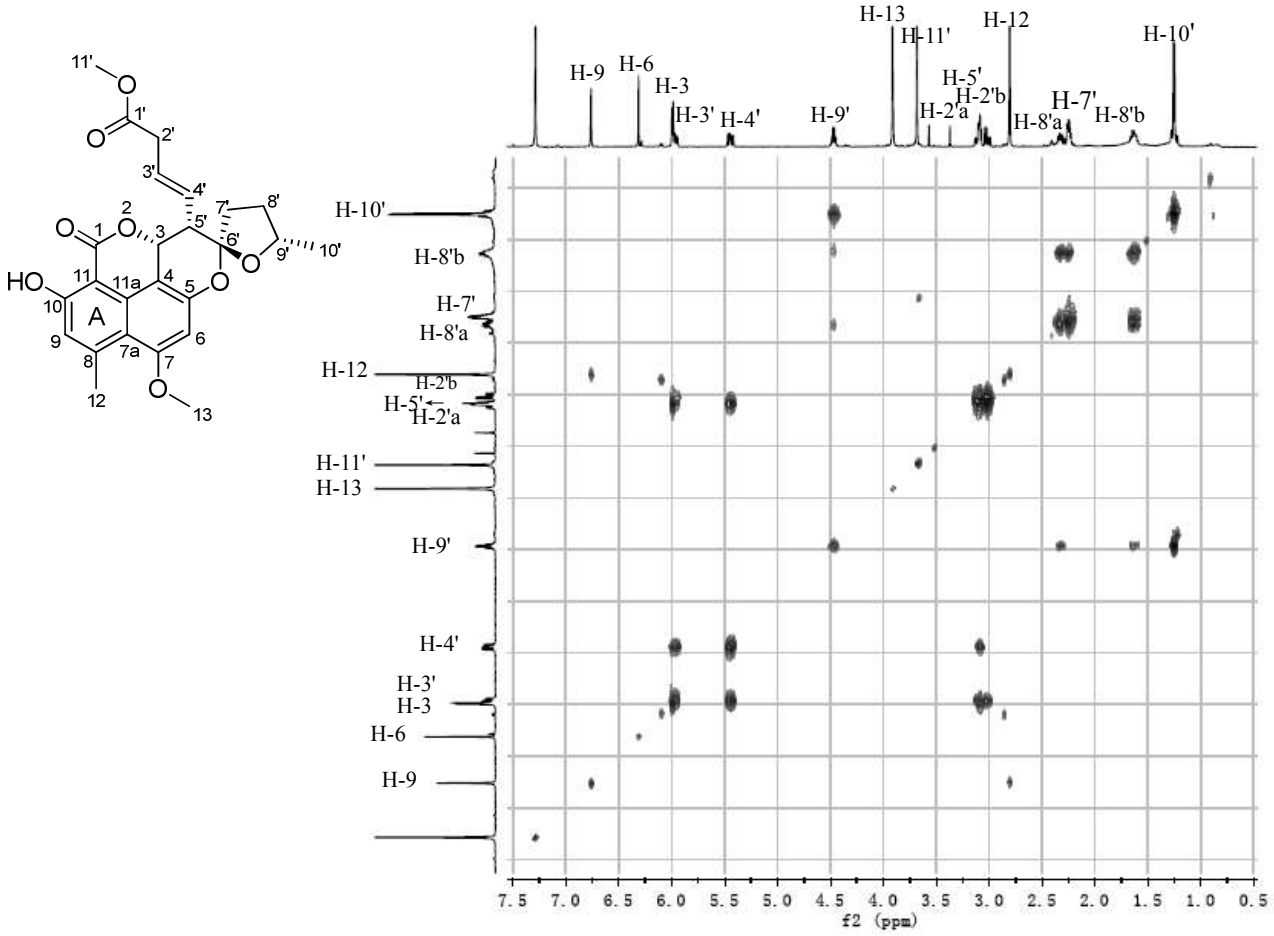

Figure S4. HSQC Spectrum of Neonectrolide A (**1**; 500 MHz, $CDCl_3$)

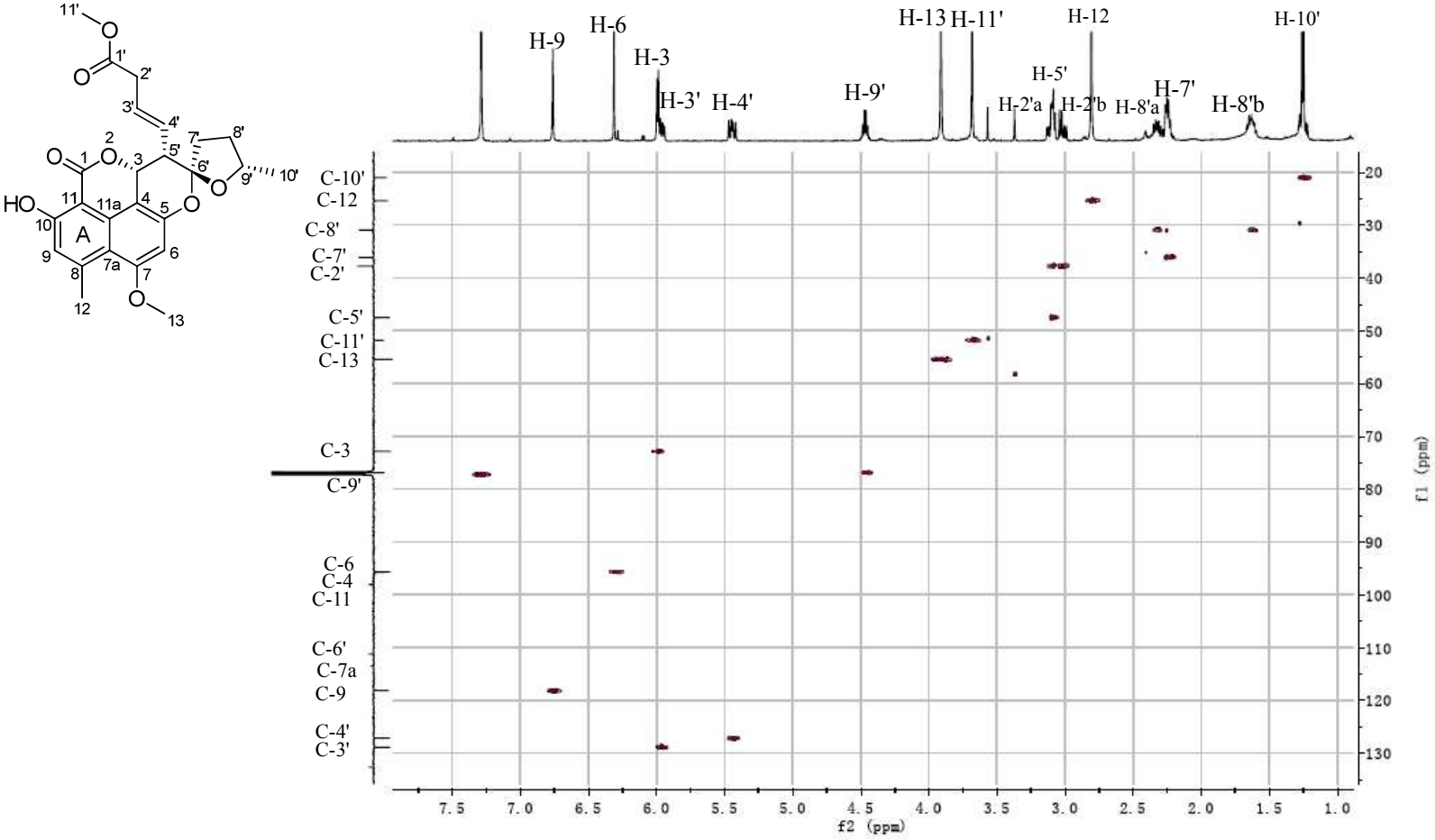

Figure S5. HMBC Spectrum of Neonectrolide A (**1**; 500 MHz, $CDCl_3$)

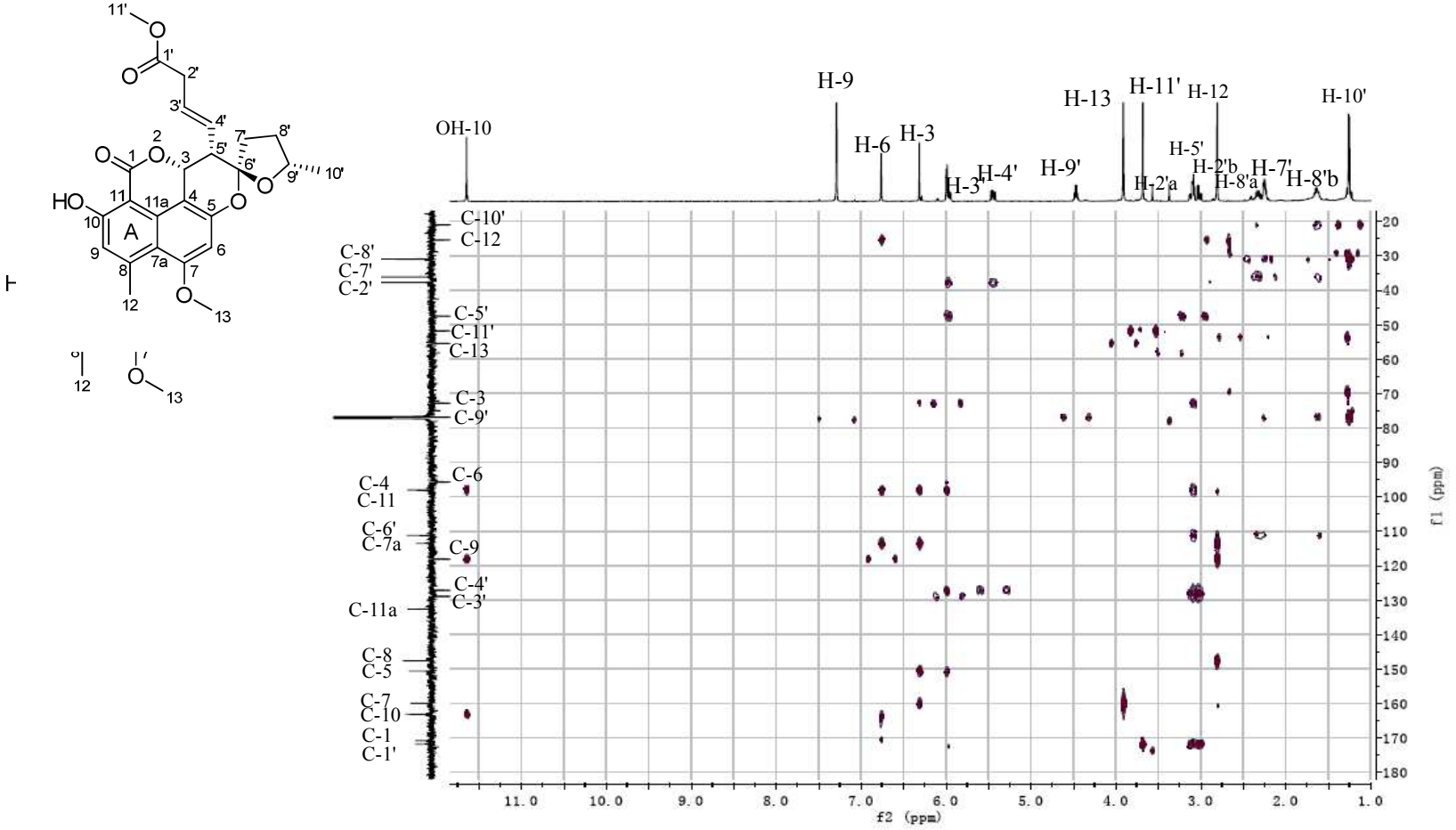

Figure S6. NOESY Spectrum of Neonectrolide A (**1**; 500 MHz, $CDCl_3$)

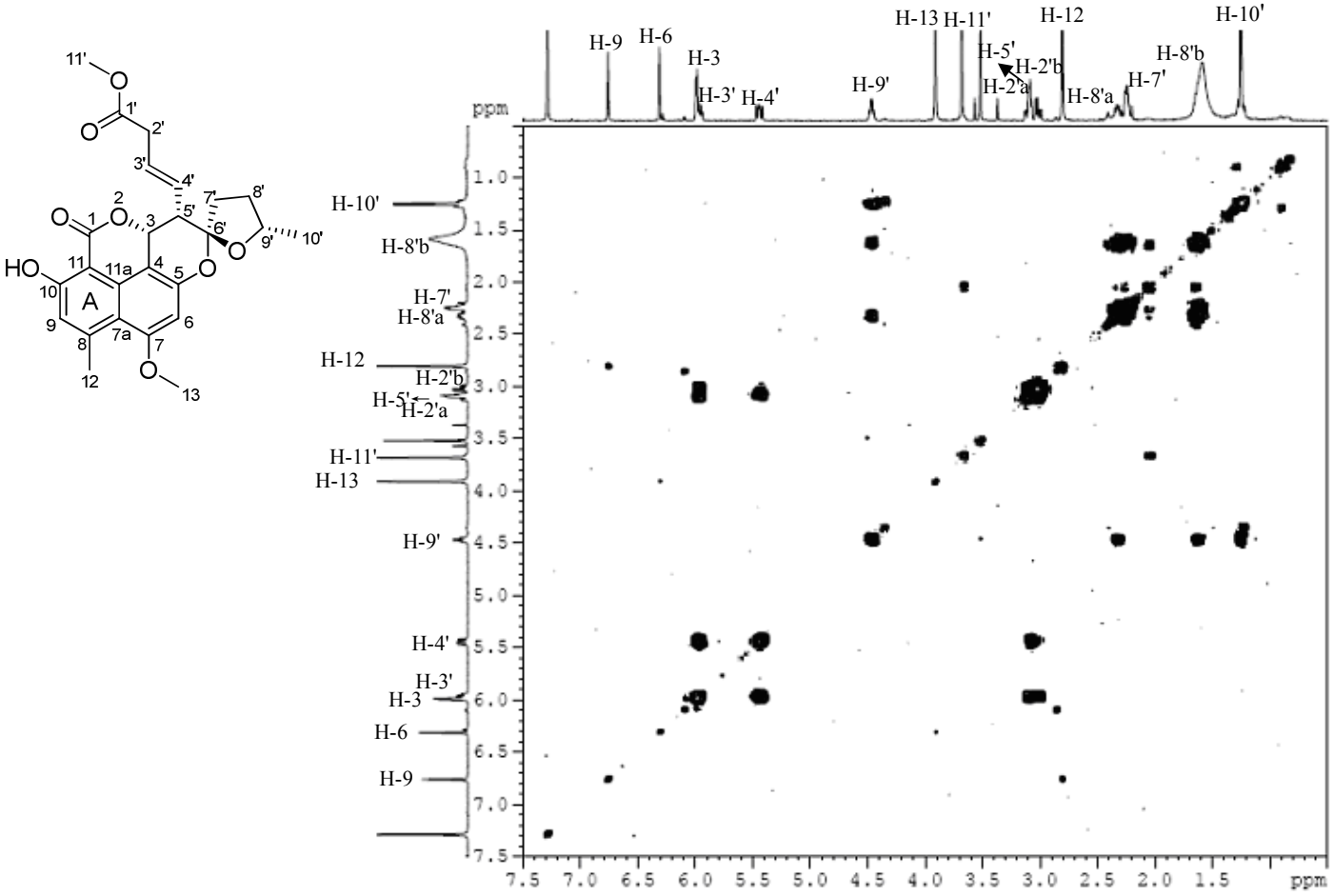

Figure S7. HRESI Spectrum of Neonectrolide A (**1**)

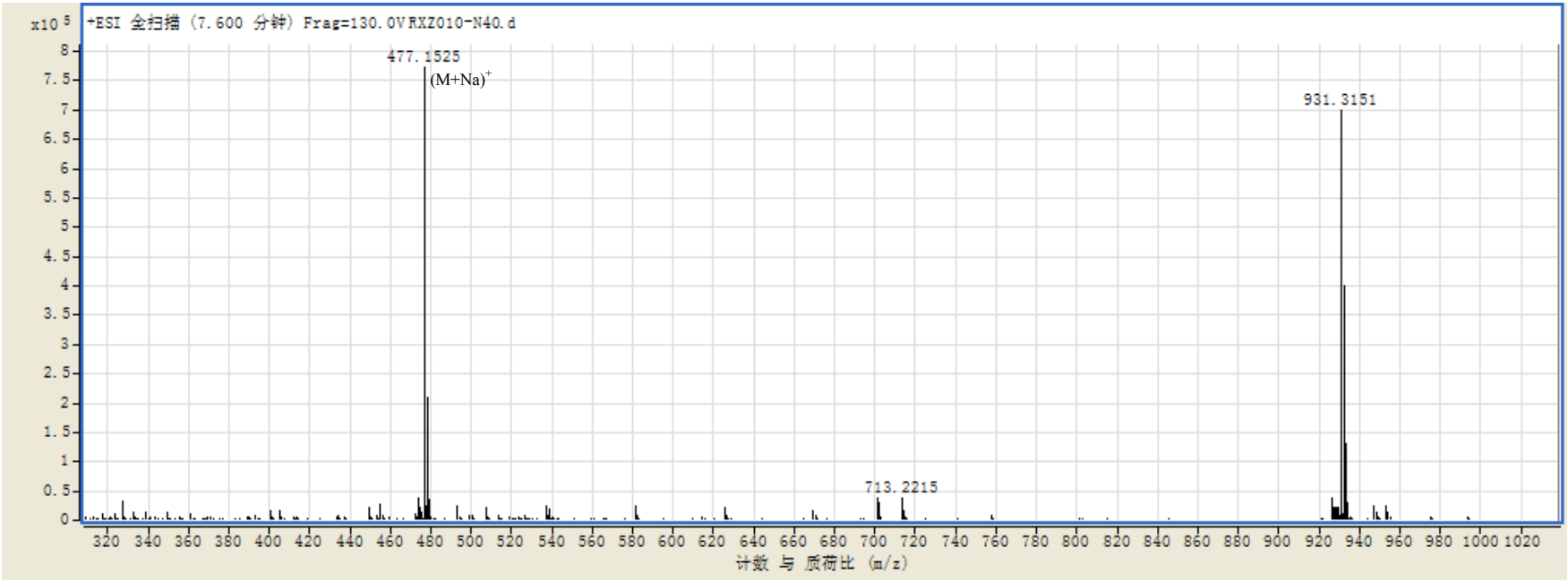

Figure S8. ^{1}H NMR Spectrum of Corymbiferan Lactone E (**2**; 500 MHz, Acetone-d_6)

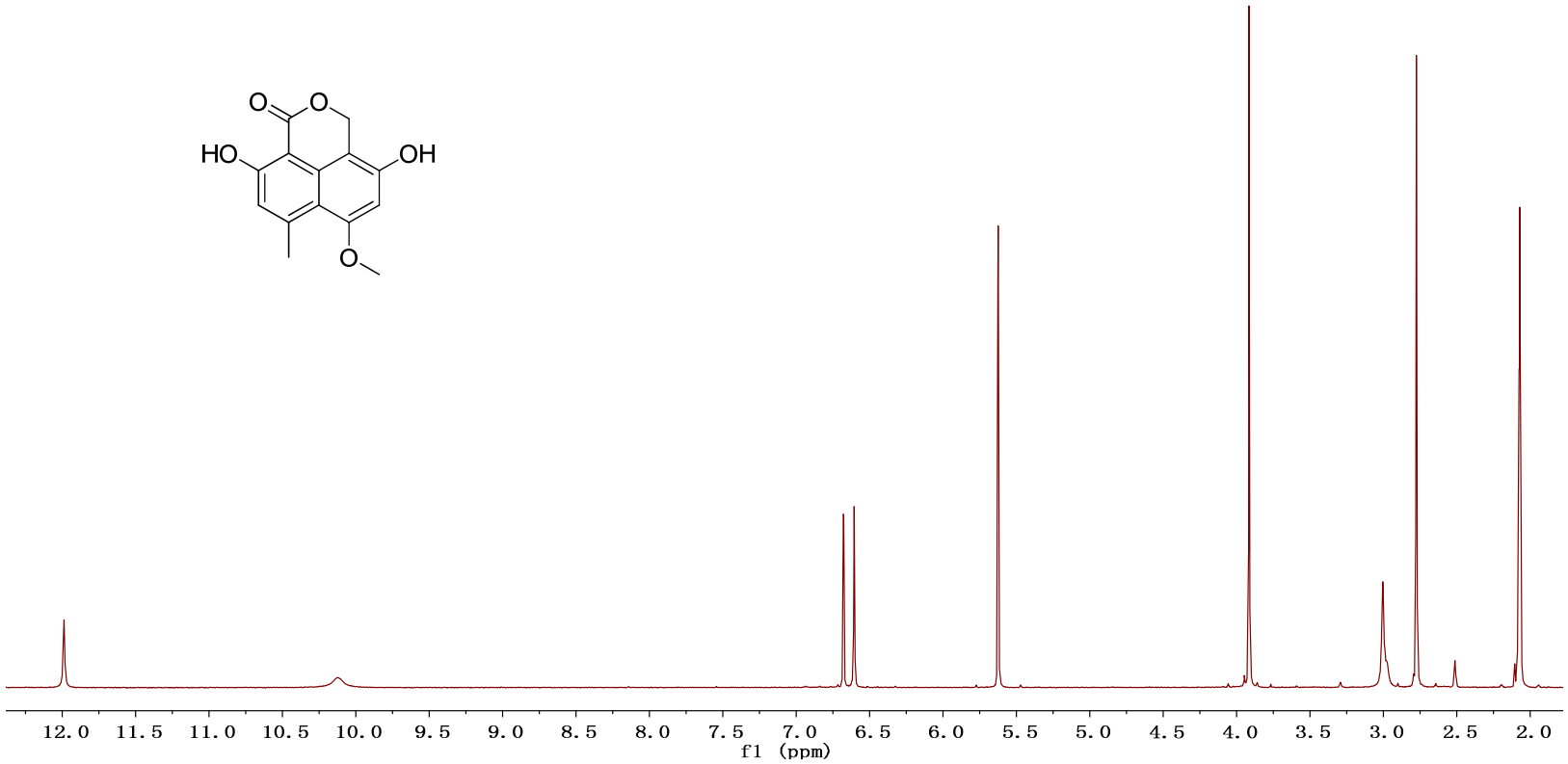

Figure S9. ^{13}C APT NMR Spectrum of Corymbiferan Lactone E (**2**; 125 MHz, Acetone-d_6)

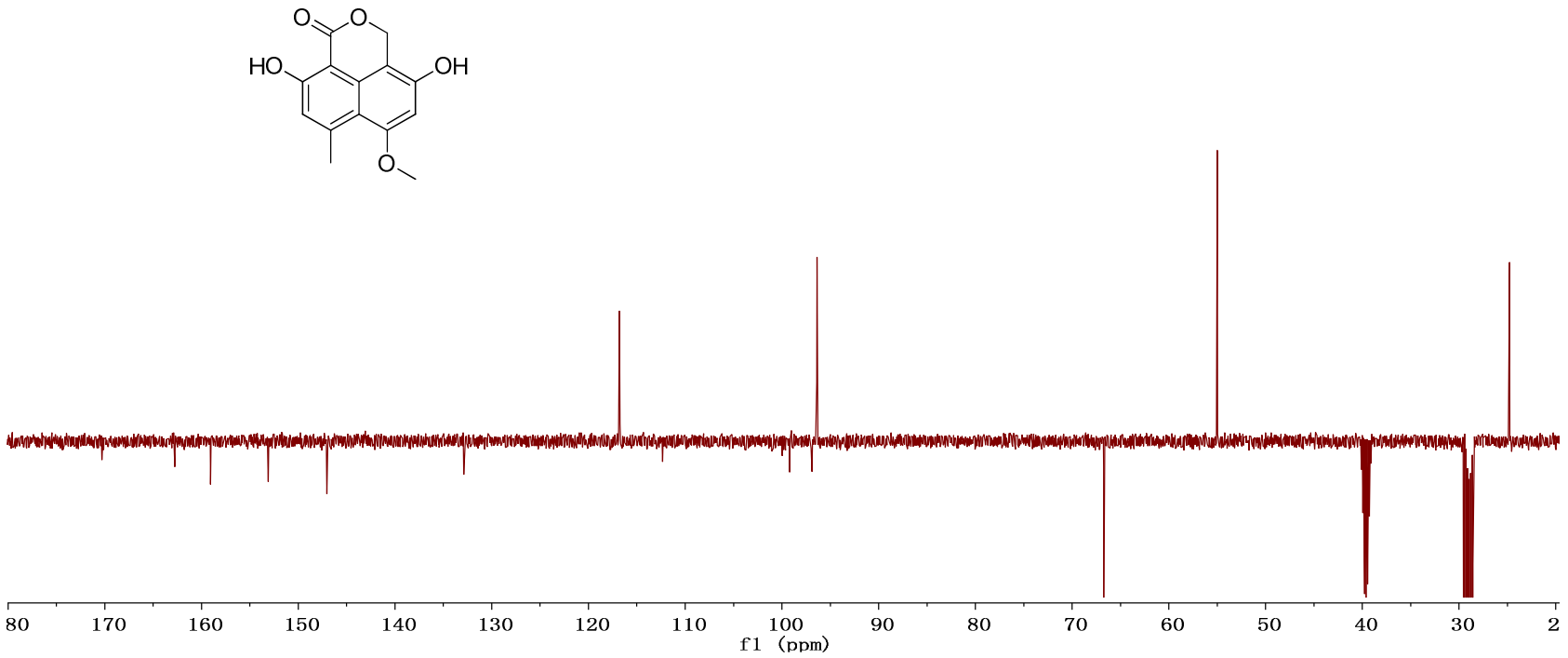

Figure S10. HMBC Spectrum of Corymbiferan Lactone E (**2**; 500 MHz, Acetone-d_6)

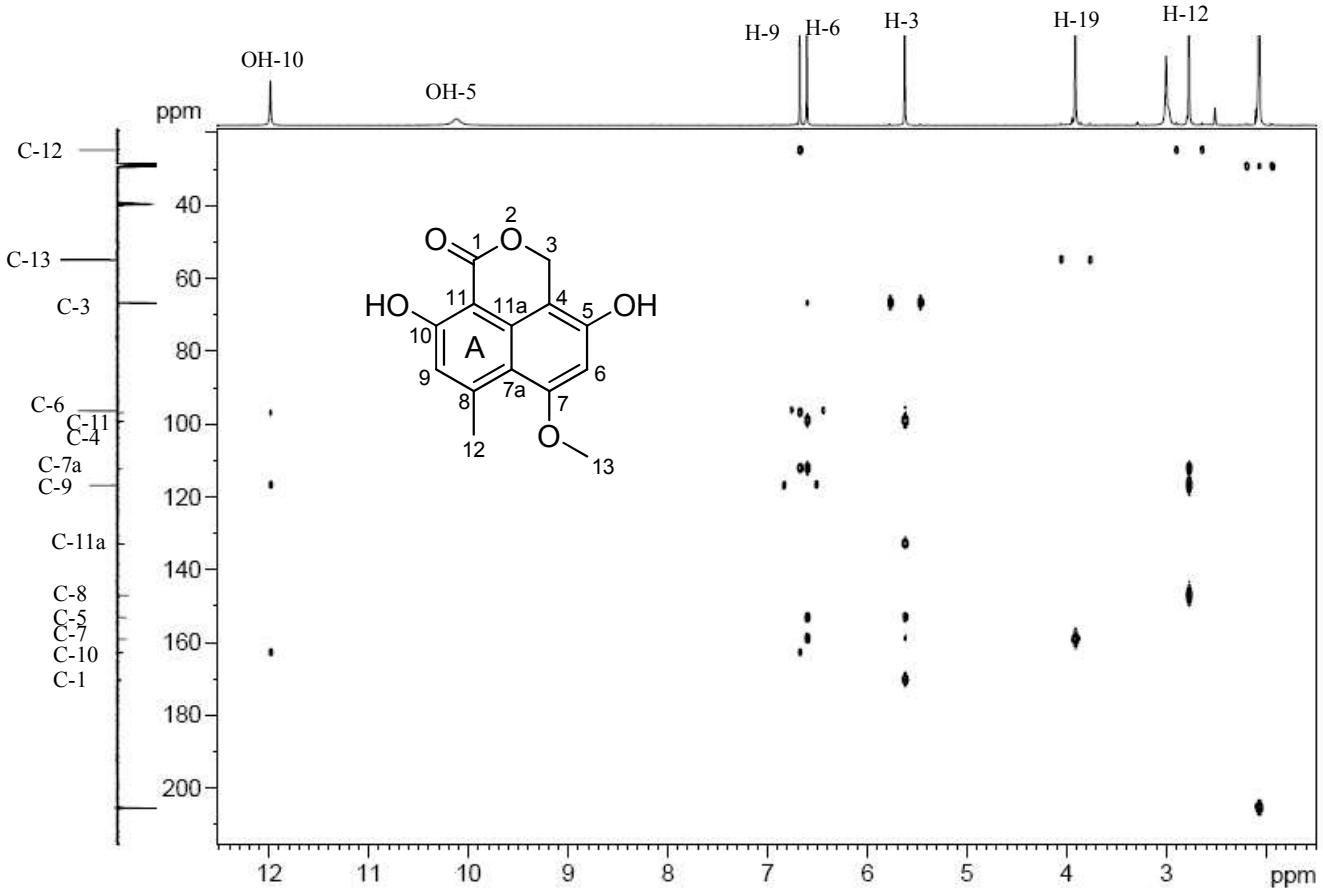

Figure S11. HRESIMS Spectrum of Corymbiferan Lactone E **(2)**

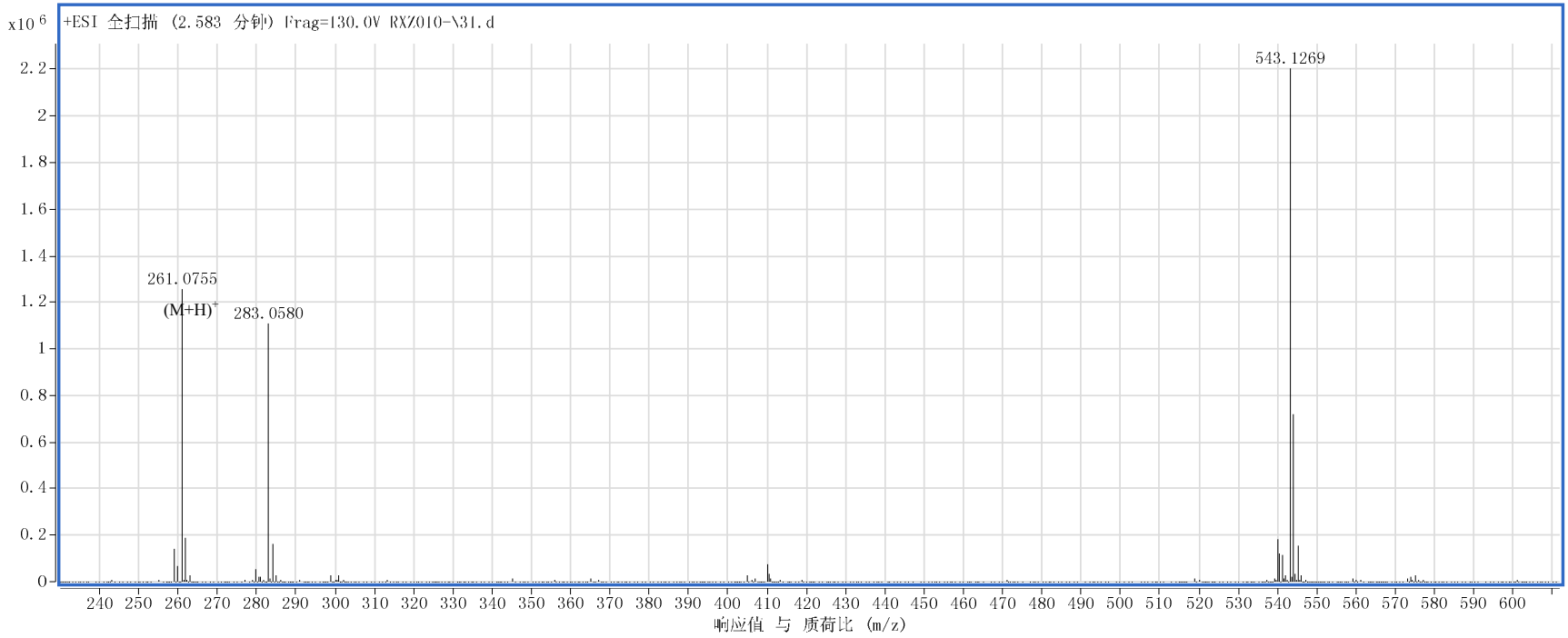

Figure S12. ^{1}H NMR Spectrum of 3-Dehydroxy-4-*O*-acetylcephalosporolide C (**3**; 500 MHz, $CDCl_3$)

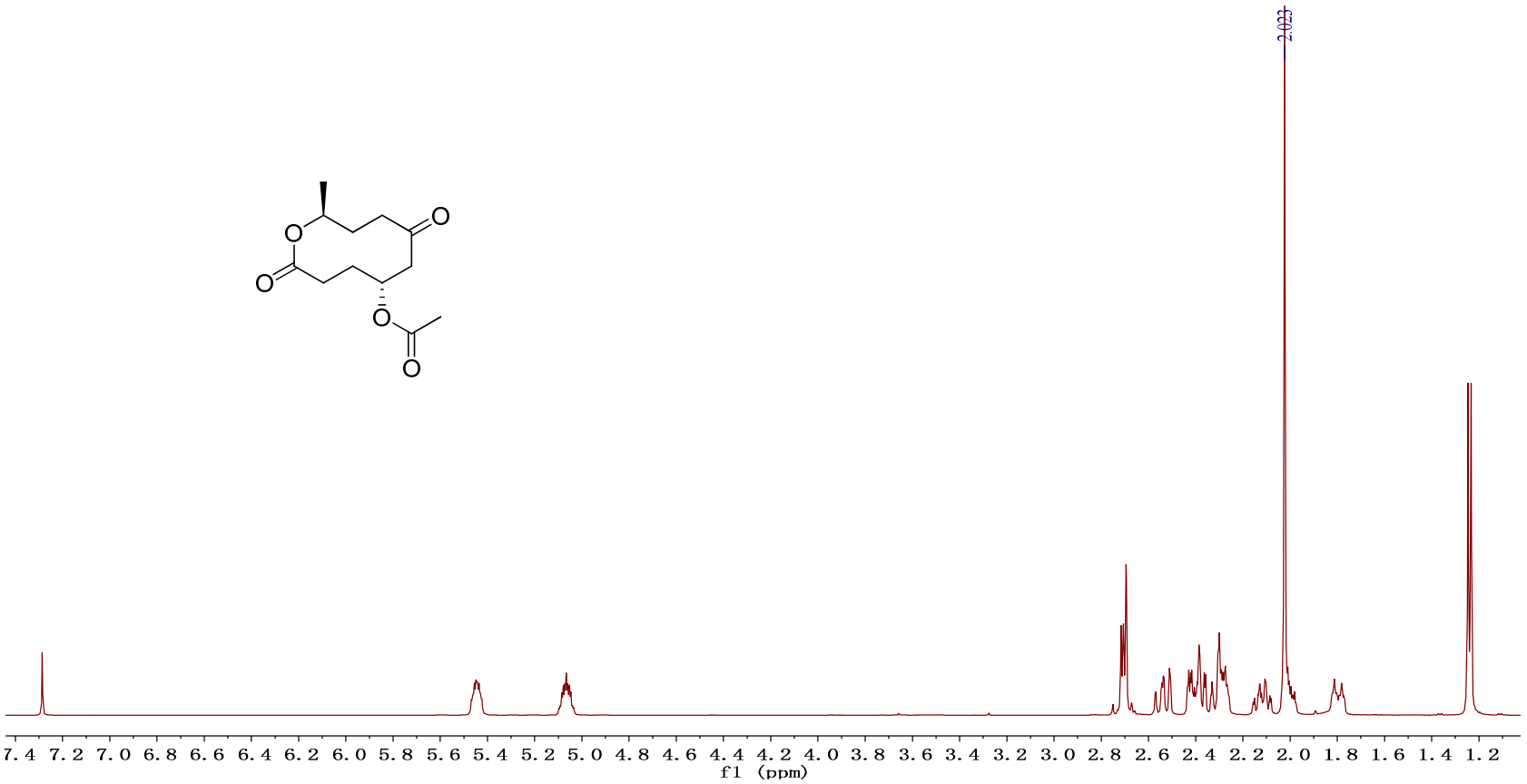

Figure S13. ^{13}C APT NMR Spectrum of 3-Dehydroxy-4-*O*-acetylcephalosporolide C (**3**; 125 MHz, $CDCl_3$)

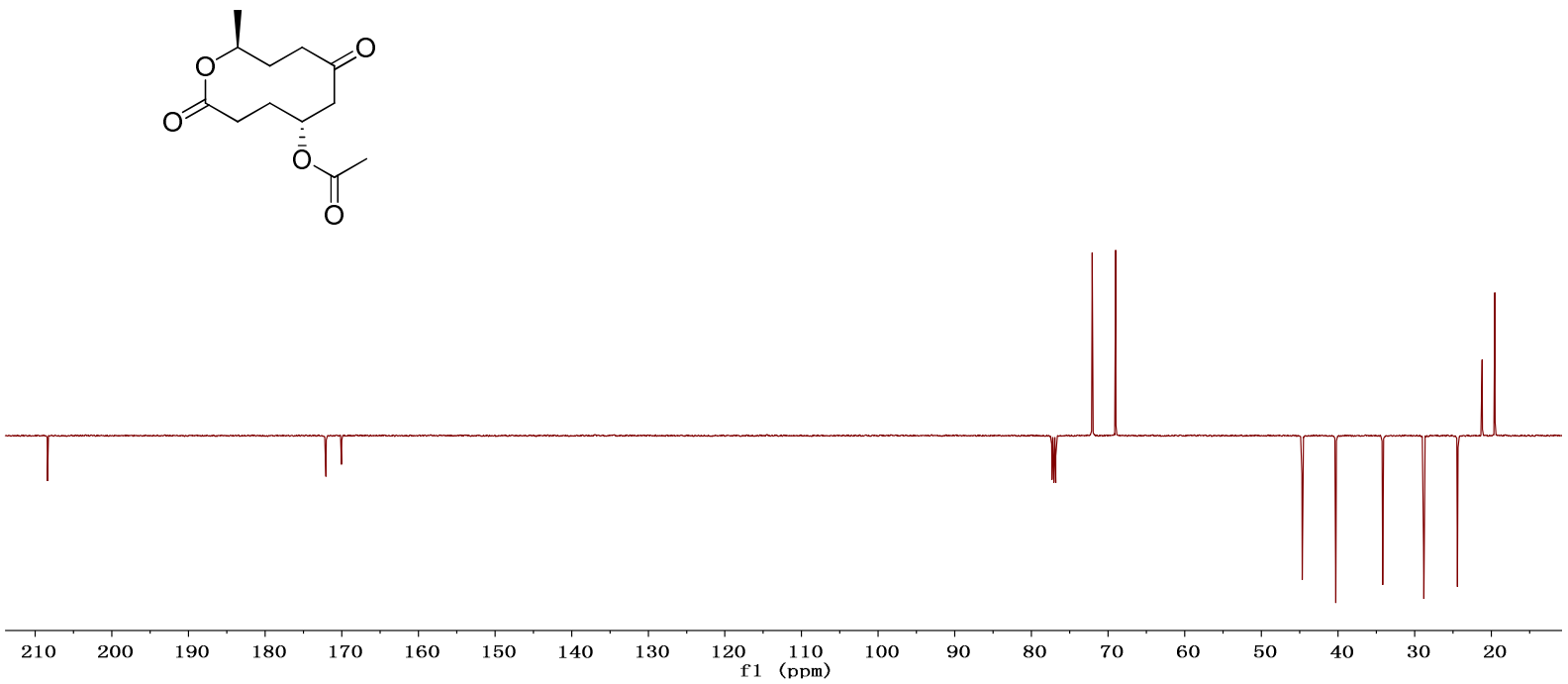

Figure S14. HMBC Spectrum of 3-Dehydroxy-4-*O*-acetylcephalosporolide C (**3**; 500 MHz, $CDCl_3$)

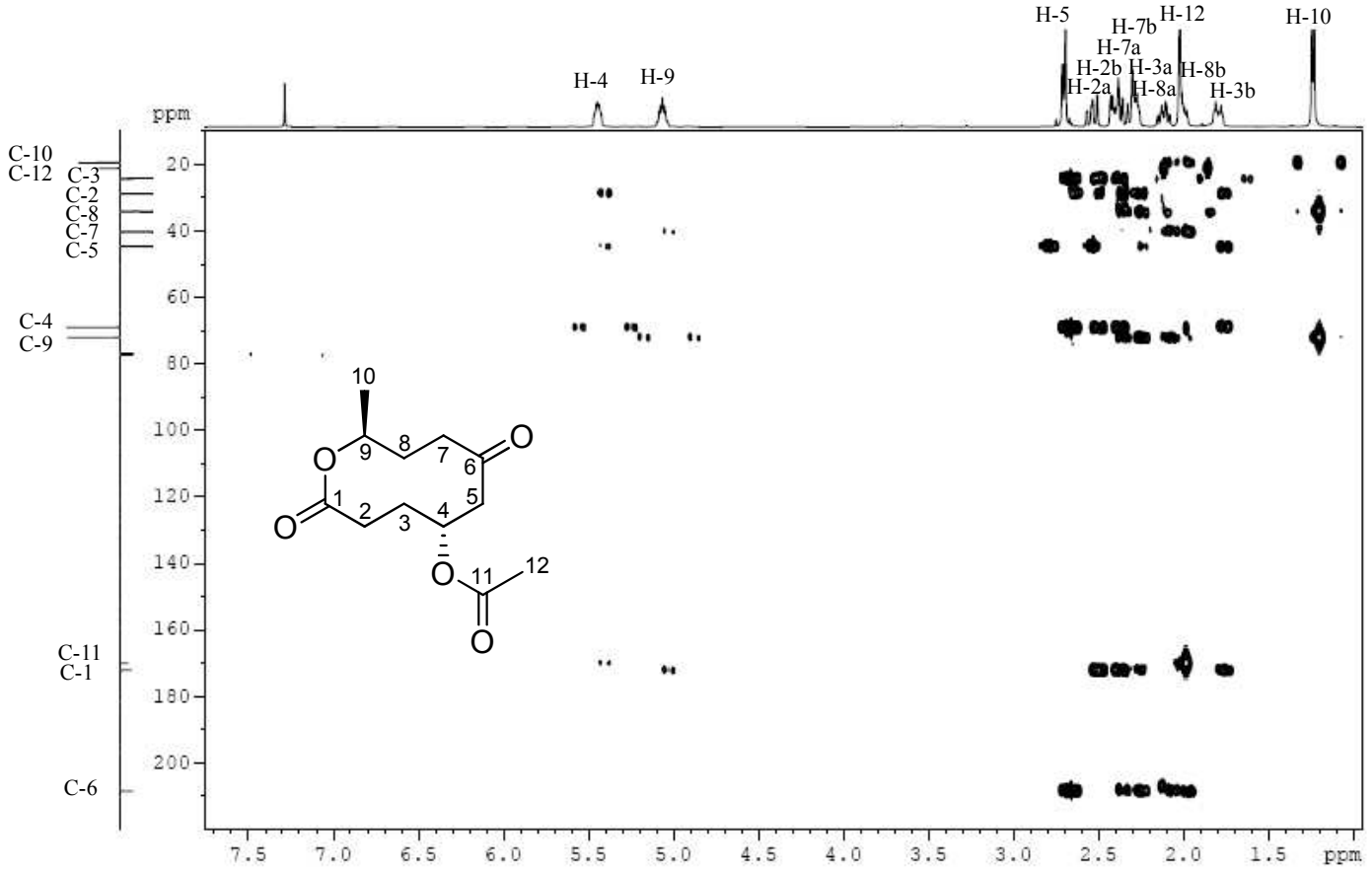

Figure S15. NOED Spectrum of 3-Dehydroxy-4-*O*-acetylcephalosporolide C (**3**; 500 MHz, $CDCl_3$)

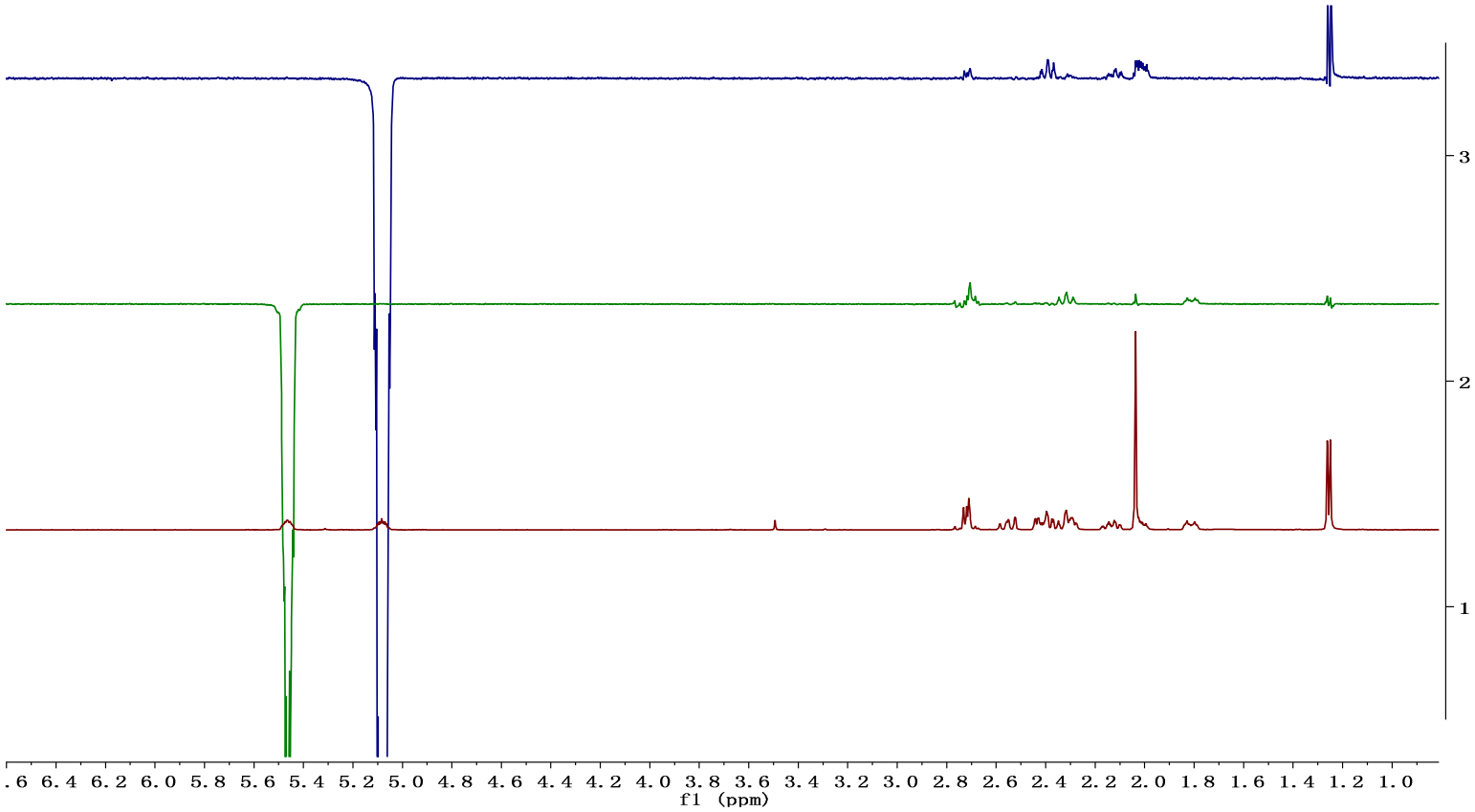

Figure S16. HRESIMS Spectrum of 3-Dehydroxy-4-*O*-acetylcephalosporolide C (**3**)

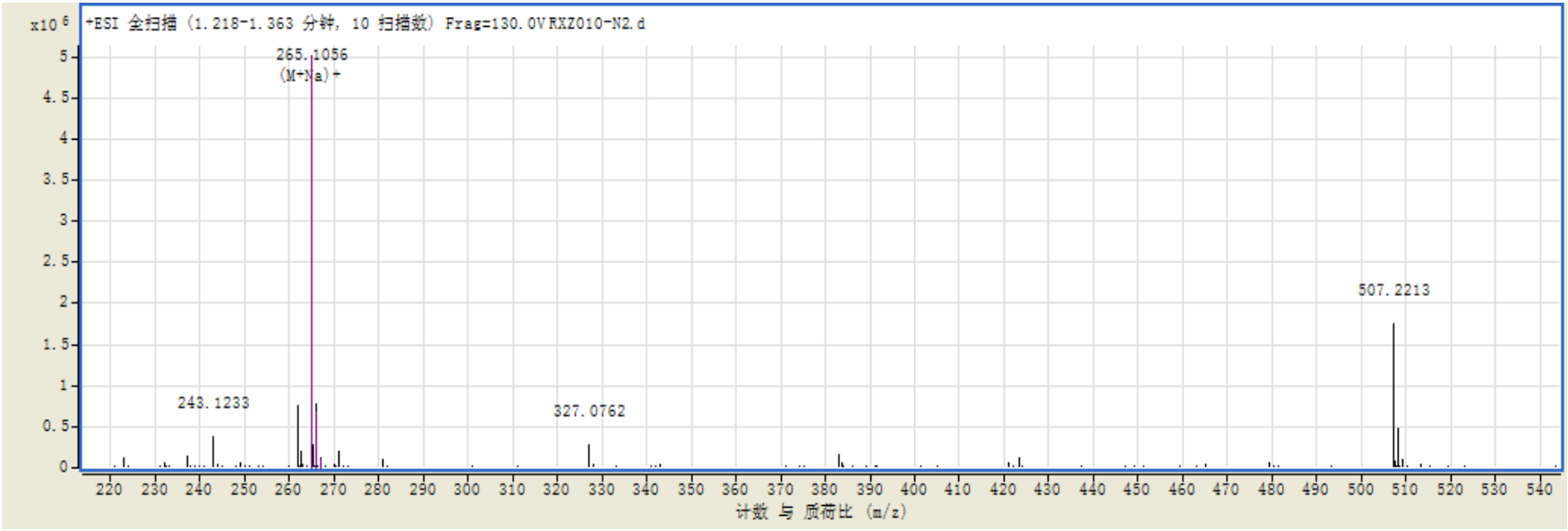

Figure S17. ^{1}H NMR Spectrum of **5a** (500 MHz, $CDCl_3$)

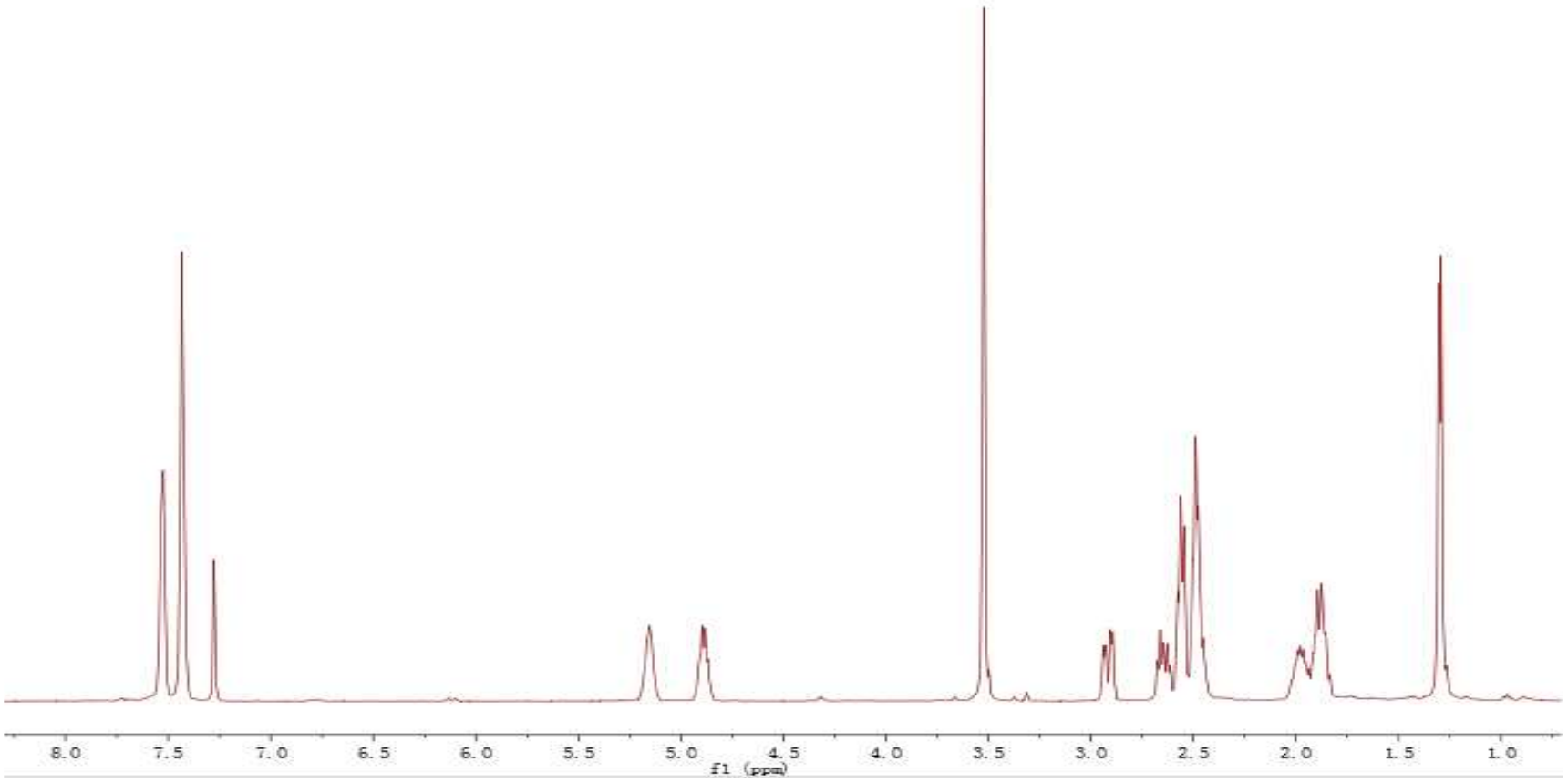

Figure S18. $^{1}H–^{1}H$ COSY Spectrum of **5a** (500 MHz, $CDCl_3$)

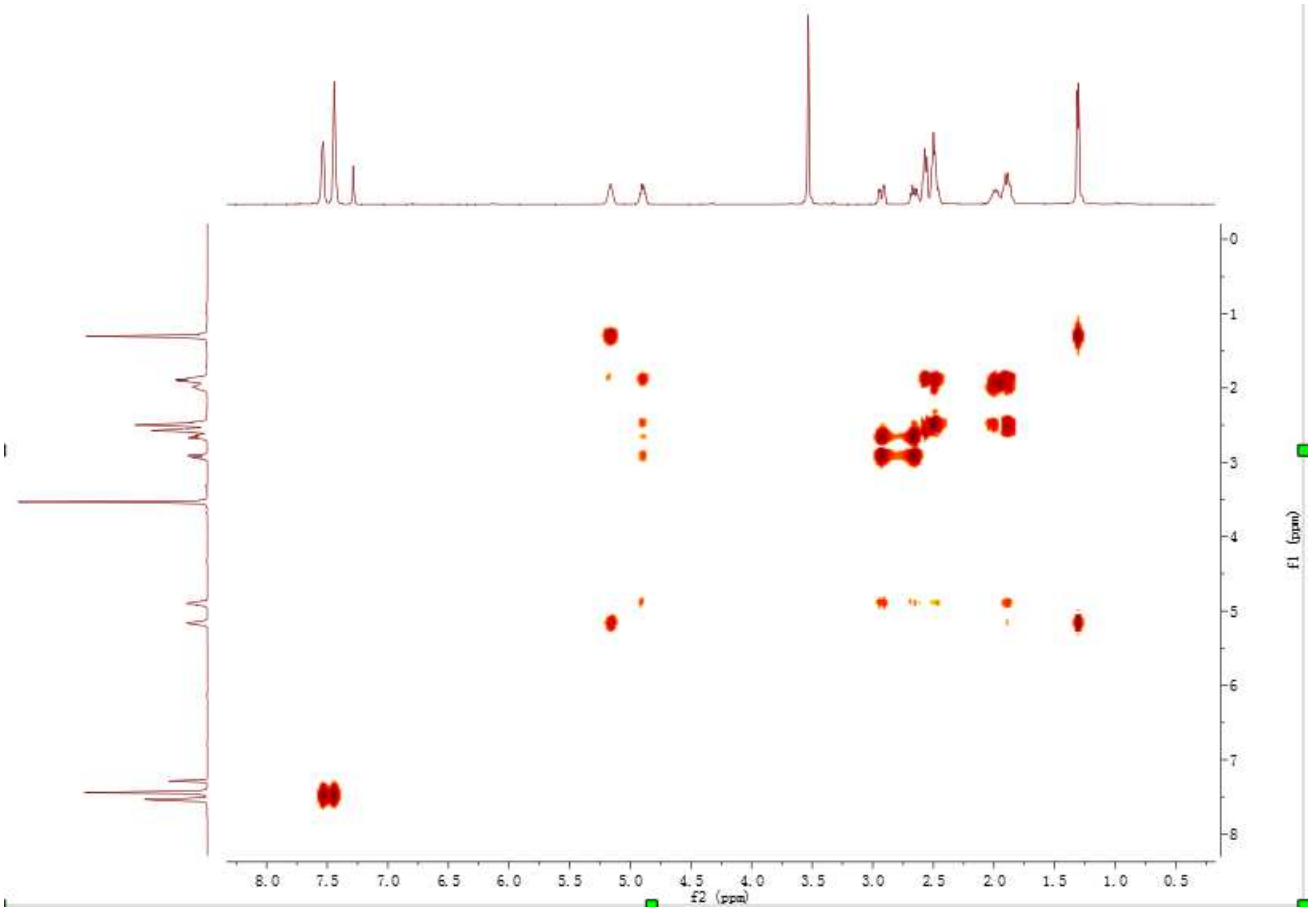

Figure S19. ^{1}H NMR Spectrum of **5b** (500 MHz, $CDCl_3$)

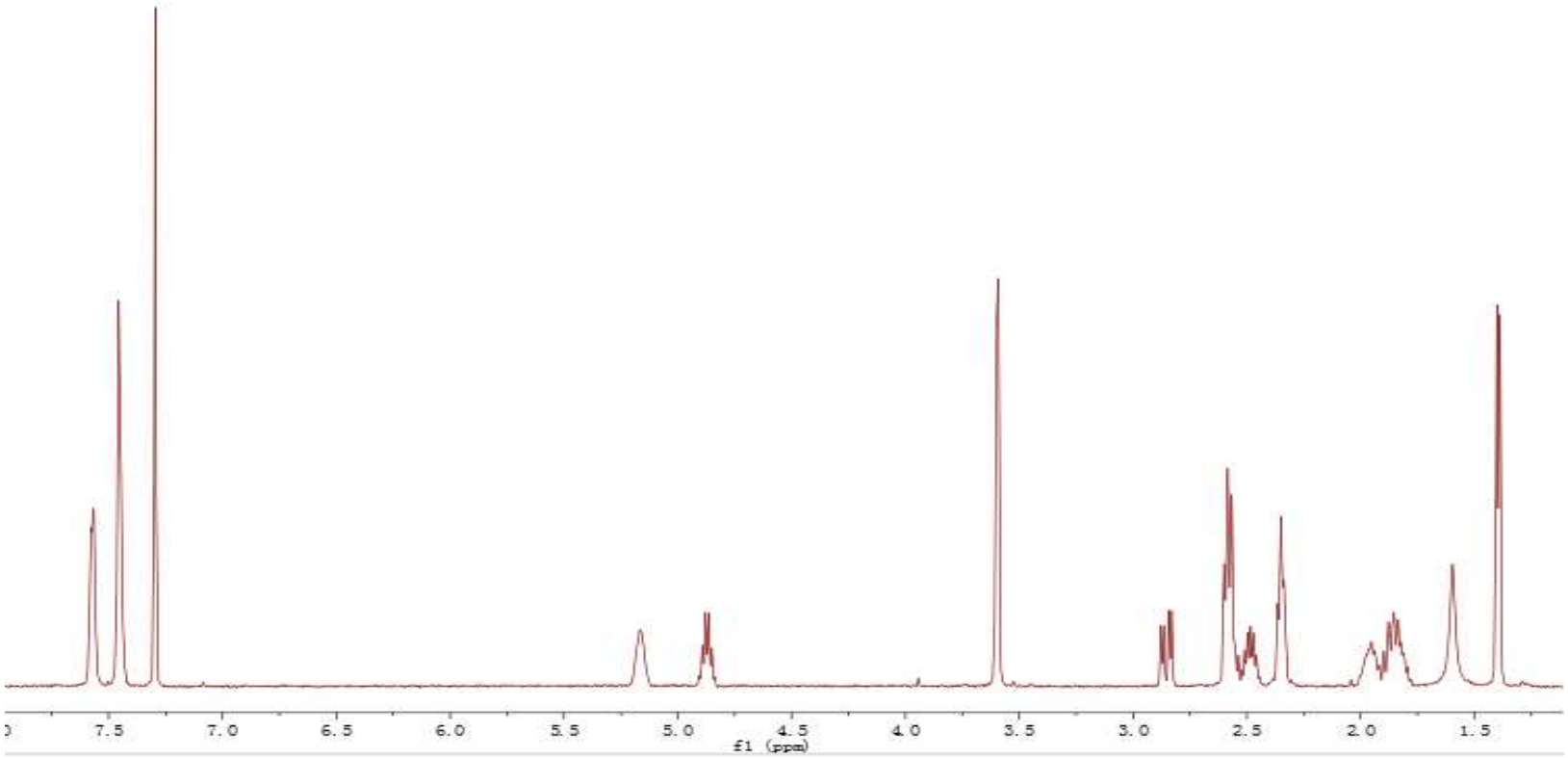

Figure S20. $^{1}H–^{1}H$ COSY Spectrum of **5b** (500 MHz, $CDCl_3$)

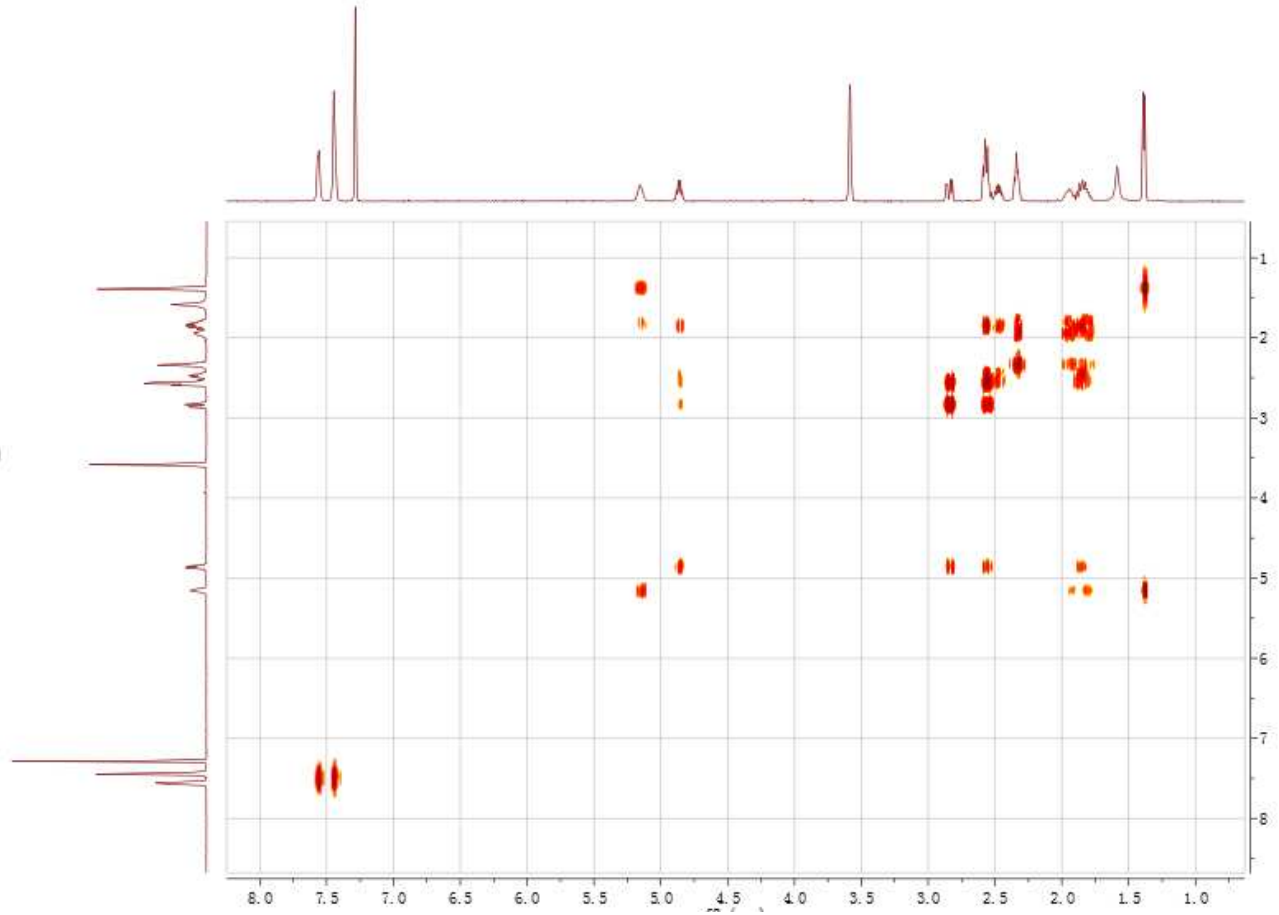

Figure S21. The Optimized Conformers for Enantiomers **4a** and **4b**

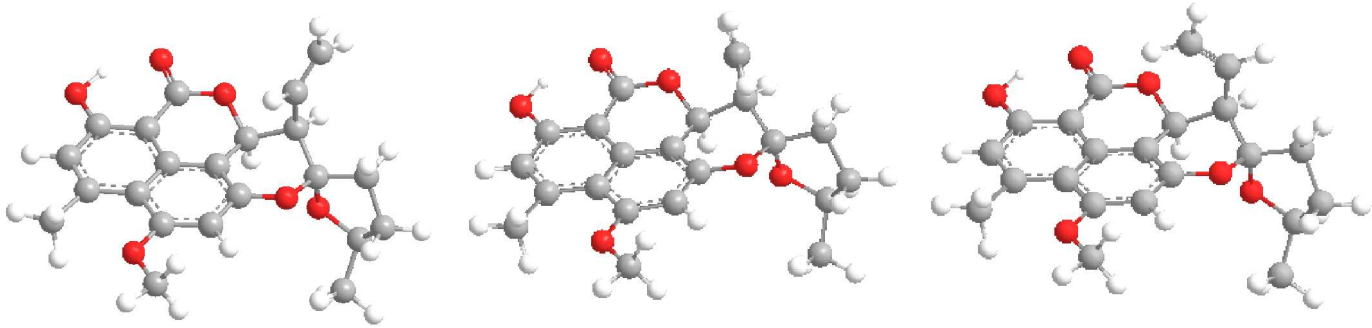

Con 1 (98.8%)

H_3–C_3–$C_{5'}$–$H_{5'}$ = 47.0°

Con 2 (0.8%)

H_3–C_3–$C_{5'}$–$H_{5'}$ =45.4°

Con 3 (0.4%)

H_3–C_3–$C_{5'}$–$H_{5'}$ = 46.1°

Figure S22. The Optimized Conformers for Enantiomers **4c** and **4d**

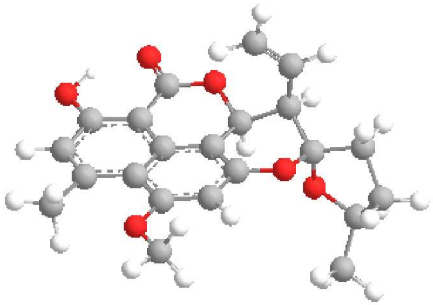

Con 1 (15.2%)

H_3–C_3–$C_{5'}$–$H_{5'}$ = 173.4°

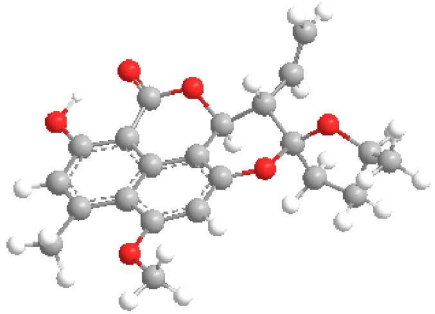

Con 2 (84.8%)

H_3–C_3–$C_{5'}$–$H_{5'}$ = 174.7°

Figure S23. The Calculated UV Spectrum of **4** and the Measured UV Spectrum of **1**

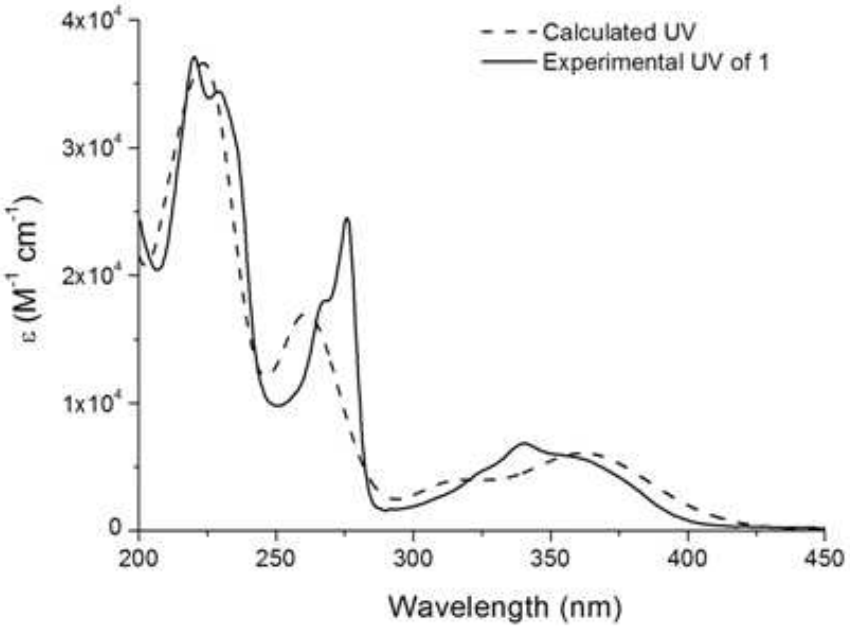

Figure S24. Molecular Orbitals Involved in Key Transitions Generating the ECD Spectrum of the Optimized Conformer of (3*R*, 5'*S*, 6'*S*, 9'*S*)-**4**

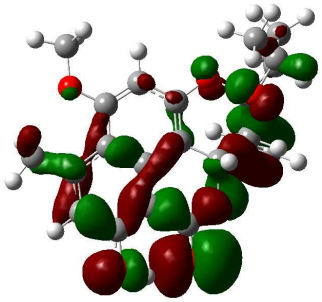
MO96

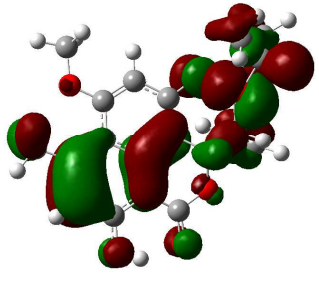
M097

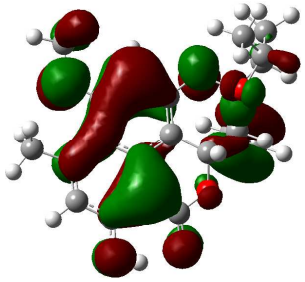
M098

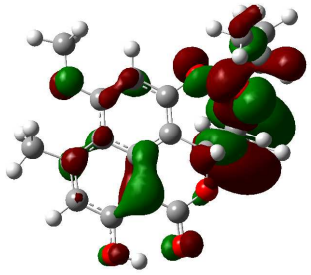
MO99

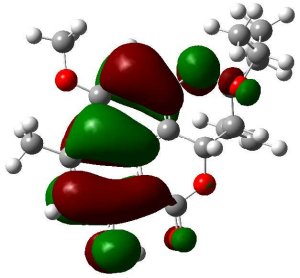
MO100

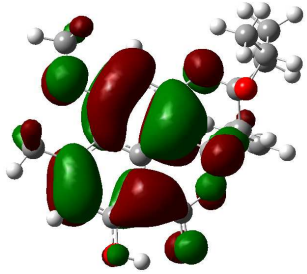
MO101

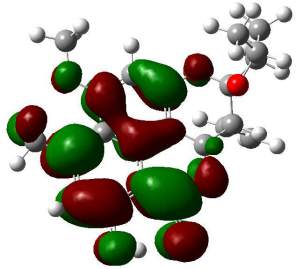
MO102

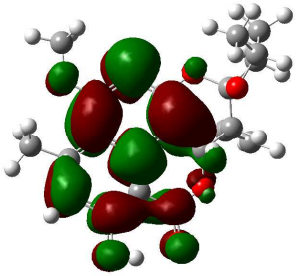
MO103

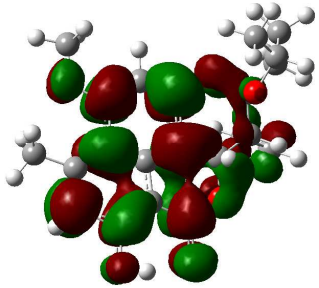
MO104

Figure S25. $\Delta\delta$ Values (in ppm) = $\delta_S - \delta_R$ Obtained for the (*S*)- (**5b**) and (*R*)-MTPA (**5a**) Esters of **5**

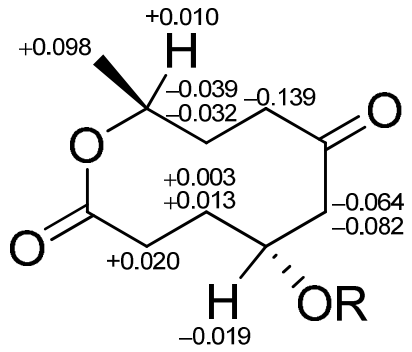

5 R = H
5a R = (*R*)-MTPA ester
5b R = (*S*)-MTPA ester

Table S1. The Optimized Structural Information for (3*R*, 5'*S*, 6'*S*, 9'*S*)-**4**

State	XX	YY	ZZ	R (velocity) (10^{-40} cgs)
1	31.4805	55.4352	–42.4971	14.8062
2	34.1961	6.5906	–49.1641	–2.7925
3	37.2459	91.1026	–88.3787	13.3232
4	–42.2222	–37.4335	28.4953	–17.0535
5	0.1733	–6.2729	12.0566	1.9857
6	–37.9541	–3.6829	–22.4069	–21.3471
7	9.7485	1.4485	–2.9799	2.7390
8	–22.9335	–32.2050	–12.5614	–22.5666
9	–36.8846	–18.3686	19.7373	–11.8386
10	11.9715	51.0995	–28.9512	11.3733
11	20.1137	3.8537	–5.7461	6.0738
12	–7.2881	–27.5528	76.9212	14.0268
13	–1.6489	1.4573	21.5256	7.1113
14	–9.8840	–6.0650	–70.4518	–28.8003
15	–23.0171	8.1690	0.8760	–4.6574
16	29.6923	0.9129	–18.1588	4.1488
17	–59.5163	34.1989	–55.7374	–27.0183
18	–23.2292	–14.8296	22.8051	–5.0845
19	22.4218	11.2675	–39.0395	–1.7834
20	26.4312	3.6375	17.1775	15.7488

Table S2. Key Transitions and Oscillator Strengths of the Optimized Conformer of (3*R*, 5'*S*, 6'*S*, 9'*S*)-**4**

Exicited State	Excitation energy (eV)	Wavelength (nm)	Oscillator Strength *f*	Dominant Contributions
1	3.4113	363.45	0.1188	101→102 0.69640
3	4.7317	262.03	0.3210	100→102 25056
				100→103 –0.11317
				100→104 –0.22352
				101→103 0.59617
4	4.8616	255.03	0.0215	100→103 0.28290
				100→104 0.12099
				101→103 0.12845
				101→104 0.60375
6	4.9941	248.26	0.0106	95→102 0.12757
				96→102 0.38151
				98→102 0.37972
				99→102 0.41065
7	5.0958	243.31	0.0040	95→102 –0.20670
				96→102 –0.34932
				98→102 0.54608
				99→102 –0.11599
8	5.2240	237.34	0.0173	97→102 0.10314
				100→103 0.13564
				101→105 0.67010
9	5.2948	234.16	0.0363	97→102 0.61705
				100→103 0.22385
				100→104 –0.12082
				101→104 –0.10538
				101→105 –0.14484